

Effect of Discharge Coefficient on Performance of Multi Jet Pelton Turbine Model

Vishal Gupta¹, Dr. Vishnu Prasad² and Dr. Ruchi Khare³

¹(Department of Energy, M.A. National Institute of Technology, Bhopal- 462003, India)

^{2,3}(Department of Civil Engineering, M.A. National Institute of Technology, Bhopal- 462003, India)

Abstract: The conversion of hydraulic energy into mechanical energy takes place in hydraulic turbines. Further this energy is converted to electrical energy with the help of generators and then supplied to consumer. With increasing demand, efficiency of every machine plays vital role. When water is stored at very high head, hydraulic energy can be converted efficiently into mechanical energy with the help of Pelton turbine. The performance of Pelton turbine at designed and off-design points is important. Performance of turbo-machines is generally evaluated before installation with the help of model testing at designed and off design regimes. Now-a-days with advanced computers and numerical techniques, Computational Fluid Dynamics (CFD) has emerged as boon for optimisation of turbo-machines. In present work, performance analysis of existing six jet Pelton turbine at design and off design discharge has been numerically carried out using Ansys-CFX. The efficiency results are compared with available model test result and found to have close comparison. The variation in pressure distribution, water velocity and water distribution have also been obtained and discussed.

Keywords: Pelton turbine, computational fluid dynamics, , pressure distribution, performance analysis

I. Introduction

Pelton turbine is used for high head for converting hydraulic energy into mechanical energy. In this turbine, the discharge required is comparatively low. Penstock conveys water from head race to distributor fitted with nozzle. The nozzle converts all the available energy of water into kinetic energy of jet [1]. Number of nozzles depends on specific speed of turbine. As number of nozzle increases, diameter of runner decreases. [2]. The force of water jet on buckets is tangential and it produces torque on shaft due to which runner rotates. Buckets have double hemispherical shape. The rear of bucket is designed such that water leaving the bucket should not interfere with the jet of water to preceding bucket [3]. The performance analysis of turbine is an important aspect to analyze its suitability under different operating conditions[4].

The most common method for assessing performance of turbines is model testing but with advances in mathematics and computational facility, CFD has emerged as cost effective tool [5] for detailed flow analysis in terms of local flow parameters and also the overall performance of turbine can be evaluated. The design of machine can be altered for the best performance.

Initially, only injector design optimisation and stress calculation on Pelton runner was done and it was first carried out by Francois [6]. The most detailed Computational Fluid Dynamics (CFD) analysis of rotating Pelton turbine was done by Perrig et al. [7] by considering five buckets (one-quarter of the runner) and the computed results were compared with experimental results at best efficiency point (BEP). Zoppe et al. [8] performed flow analysis inside stationary Pelton turbine bucket using commercially available CFD code Fluent and validated the results experimentally. Gupta and Prasad [9] have presented effect of jet shape on water distribution in Pelton bucket. Parkinson et al. [10] have simulated unsteady analysis of Pelton runner. Gupta et. al.[9], Patel et al. [11], Dynampally and Rao [12] have worked on effect of time step and grid refinement.

Flow in stationary flat plate was simulated by Konnur et. al. [13]. Islam et al. [14] have used composite material for manufacturing Pelton wheel and tested it. Xiao [15] and Zhang [16-17] have studied or simulated effect of friction on Pelton buckets. Zhang[18-20], Binaya et.al [21], Santolin [22] have worked for impact, flow dynamics and pressure distribution in Pelton bucket. But very few authors have worked for performance prediction of Pelton turbine at off-design regimes.

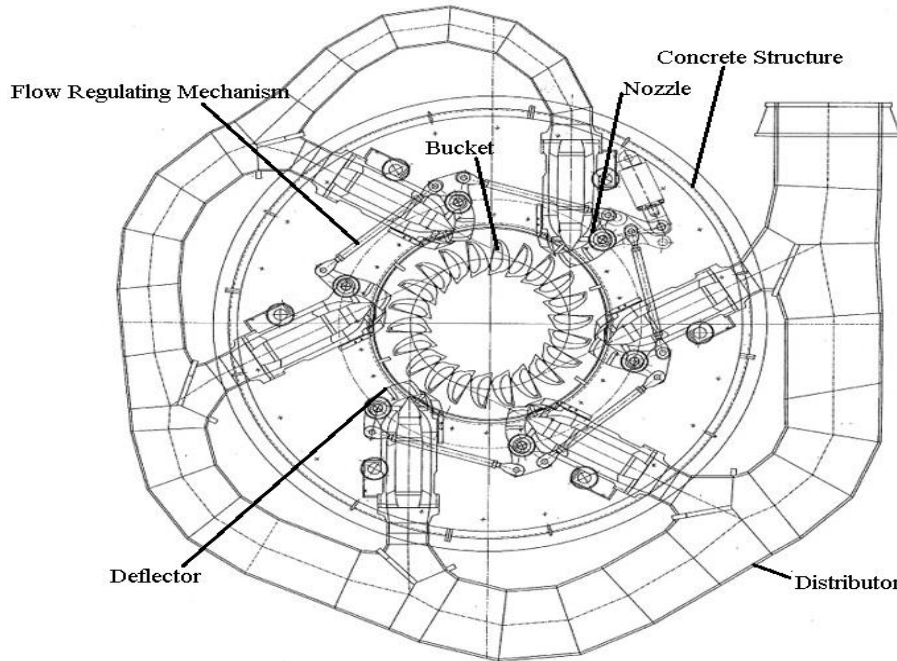


Fig.1: Parts of Pelton turbine.

In the present paper, numerical flow simulation of a six jet Pelton turbine shown in Fig.1 has been carried out to assess its performance at different discharge coefficients using commercial CFD code ANSYS CFX.

II. Governing Equations

The partial differential equations based on conservation of mass, momentum and energy are the fundamental governing equations of fluid dynamics and are known as continuity, momentum and energy equations [25, 26]. Flow having more than one working fluid is termed as multiphase flow. The water jet which leaves nozzle and hits the buckets of Pelton wheel is surrounded by air from all sides. When all working fluids have the same velocity, pressure, turbulence fields etc. except volume fractions, it is the limiting case of Eulerian- Eulerian multiphase flow and the flow may be termed as homogeneous multi phase flow. Free surface flow refers to the multi phase situation where two fluids are physically separated by distinct resolvable inter-phase [27]. The homogeneous multiphase flow is commonly used for free surface flows simulations. The governing equations for multiphase flow are given below.

Continuity Equation:

$$\frac{\partial \rho_m}{\partial t} + \vec{\nabla} \cdot (\rho_m \vec{W}_m) = 0$$

where the mixture density and the mixture relative flow velocity are defined as

$$\rho_m = \sum_{n=1}^2 \alpha_n \rho_n$$

$$\vec{W}_m = \frac{\sum_{n=1}^2 \alpha_n \rho_n \vec{W}_n}{\rho_m}$$

and

the volume fraction α_n is given by

$$\alpha_n = \frac{V_n}{\sum_{n=1}^2 V_n}$$

Momentum Equation:

$$\frac{\partial}{\partial t} (\rho_m \vec{W}_m) + \rho_m (\vec{W}_m \cdot \vec{\nabla}) \vec{W}_m = -\vec{\nabla} p_m + \vec{\nabla} (\bar{\tau}_m + \bar{\tau}_{t_m}) - \rho_m \vec{\omega} \times (\vec{\omega} \times \vec{r}_m) - 2\vec{\omega} \times \vec{W}_m + \vec{f}_m$$

III. Geometric Modeling

For numerical simulation in Pelton turbine, 3-dimensional geometry of stator and rotor are required. Pelton turbine taken for performance analysis has six jets and 20 buckets. The complete flow domain consist of stator and rotor domain. But in present simulation, stator domain from exit of nozzle to runner with only three symmetrical half jets and rotor domain with 10 symmetrical half buckets are modelled due to limitation of computational facility. The geometric models of stator and runner have been shown in Fig.2 and Fig.3.

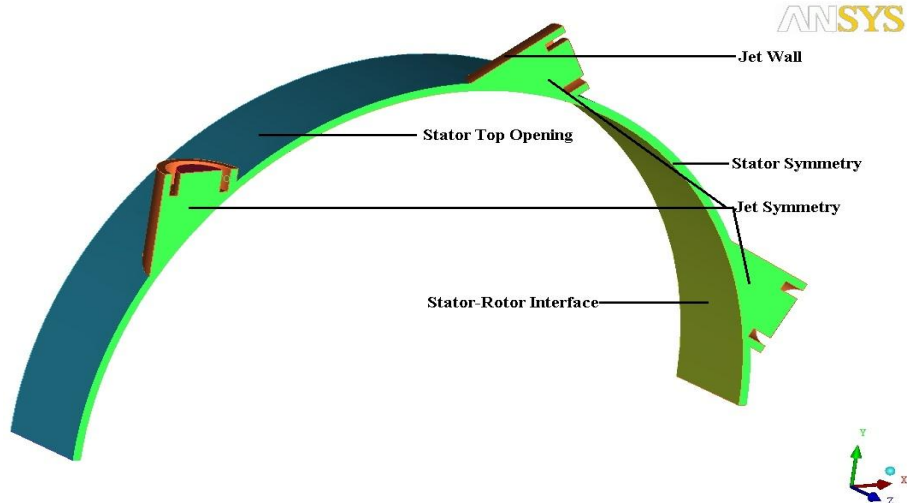


Fig.2: Geometry of stator domain

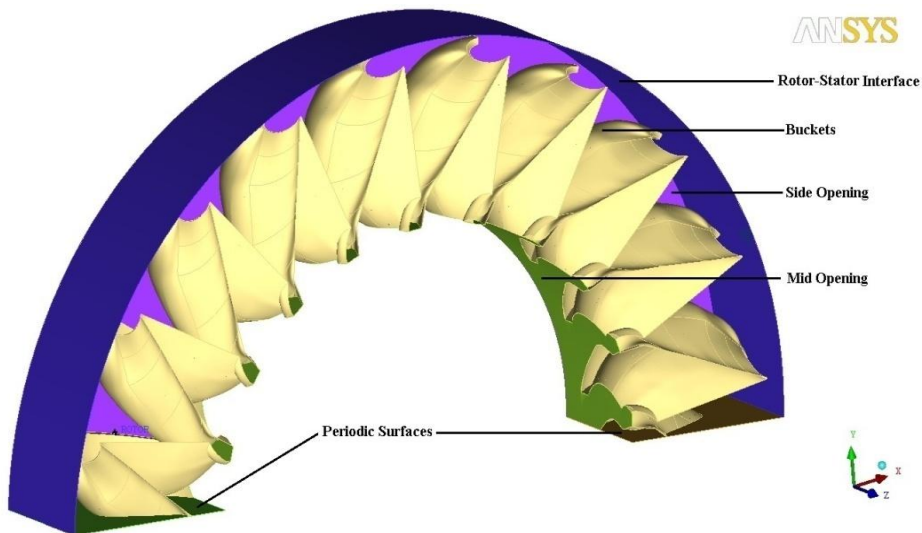


Fig.3: Geometry of rotor domain

IV. Mesh Generation

The complete flow regime is to be discretised into elements (mesh) for numerical simulation. In present case, prism and tetrahedral mesh elements for 3-D flow domain and triangular elements for surface are taken. Meshing of rotor domain is shown in Fig.4. Jet walls are applied with prism layer to capture the boundary layer flow accurately.

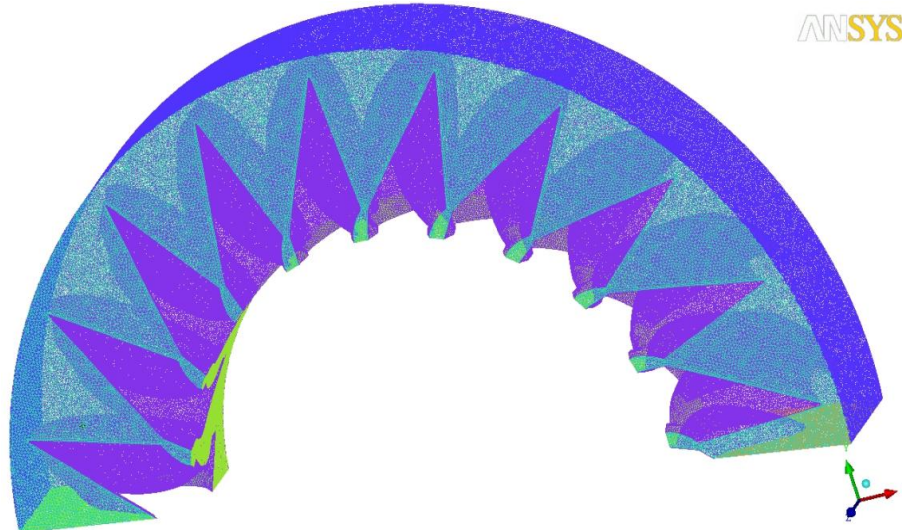


Fig.4: Meshing of rotor domain

V. Boundary Conditions

Practically the cross sectional area of nozzle is varied by movement of spear in nozzle to vary the discharge but in CFD, the diameter of jet have been varied for getting variation in discharge coefficient. The speed of rotor domain has been kept constant. Stator domain is kept stationary. SST $\kappa\text{-}\omega$ turbulence model is considered for analysis.

To obtain solution of a flow problem, flow parameters like pressure, velocity or mass flow are needed to be specified at inlet and outlet boundaries. Air and water as working fluids with reference pressure of 1 atmospheric are taken for all the cases. The flow has been simulated as transient flow condition with time step corresponding to 1° of runner rotation.

Jet inlet has been defined as inlet boundary with water velocity of 30.7 m/s normal to surface. Symmetric type boundary conditions have been applied at jet symmetry, stator symmetry, rotor symmetry. Symmetric ends of stator and rotor are defined as periodic because of limitation of computational power. As the flow around Pelton turbine is free surface flow and pressure all around the turbine is atmospheric, so opening type boundary conditions are applied at stator side opening, stator top opening, rotor side opening and rotor mid opening. Transient rotor-stator interface are applied at stator and rotor interfaces.

VI. Formulae Used

The buckets in front of jet reduces jet velocity to zero in its direction and diverts the jet at the outlet angle of bucket. The change in jet velocity produces force on bucket due to momentum change and torque on turbine shaft to rotate it. The various parameters for performance analysis are computed as:

Input power:

$$P_i = \rho \times g \times Q \times H \quad (1)$$

Output power:

$$P_o = \frac{2 \times \pi \times N \times T}{60} \quad (2)$$

Hydraulic efficiency:

$$\eta_h = \frac{P_o}{P_i} * 100 \quad (3)$$

Time step corresponding to 1° runner rotation:

$$\Delta t = \frac{60}{360 \times N} \quad (4)$$

Discharge coefficient:

$$K_Q = \phi_B = \frac{4 \times Q}{\pi \times B^2 \times Z \sqrt{2 \times g \times H}} \quad (5)$$

Discharge through one nozzle:

$$Q_1 = \frac{Q}{6} \quad (6)$$

Velocity of jet:

$$V = C_v \sqrt{2 \times g \times H} \quad (7)$$

Cross sectional area of jet:

$$A_1 = \frac{Q_1}{V} \quad (8)$$

Blade loading coefficient:

$$C_p = \frac{P}{\frac{1}{2} \rho C_1^2} \quad (9)$$

Torque coefficient:

$$K_T = \frac{T}{\rho \times U_1^2 \times B \times L \times D} \quad (10)$$

Relative velocity coefficient:

$$K_w = \frac{W}{\sqrt{2 \times g \times H}} \quad (11)$$

Absolute velocity coefficient:

$$K_c = \frac{C}{\sqrt{2 \times g \times H}} \quad (12)$$

Loss coefficient:

$$K_L = \frac{W_2}{W_1} \quad (13)$$

Normalised efficiency coefficient:

$$\delta = \frac{\text{Efficiency at point}}{\text{Maximum efficiency}} \quad (14)$$

VII. Mesh Independency Test

For obtaining solution of a flow problem numerically, mesh size and quality plays a vital role on accuracy of solution and hence the result should checked to be independent of number of mesh elements. Mesh independency test is been done by varying the mesh size. For stator mesh independency was found to be at 456,213 nodes (2,146,945 tetrahedral and 1089 pyramid elements).

For obtaining mesh independency of rotor, time step corresponding to 1° runner rotation is chosen. The total simulation is carried for 100° of Pelton runner rotation and it was found that numerical results are independent of mesh at 1,537,618 nodes. Mesh quality is found to be within recommended values of ANSYS CFX. It took about 77 hours for completion of simulation and computed efficiency is found to be 88.03% which is very close to experimental value.

VIII. Numerical Parametric Study

Numerical flow simulation results were checked for reliability and accuracy at BEP with experimental results for validation. The accuracy of simulation depends on many factors. The simulations at different parameter values have been carried out and their effect on accuracy of solution has been studied for proper selection of parameters for simulation in Pelton turbine at different operating regimes.

8.1 Study of turbulence model

The comparison in efficiency was done for standard κ - ϵ turbulence model with scalable wall function and SST κ - ω turbulence model given by Menter.

Numerically calculated efficiency for κ - ϵ turbulence with scalable wall function is found to be 85.95% and it took about 69 hours for simulation. The simulation using SST model took about 77 hours and 88.03% efficiency is obtained. SST model is able to capture turbulent scales in flow in high shear stress regions. So SST turbulence model is chosen for further simulations.

8.2 Study of time step

Time steps are interval for which CFX solver calculates flow parameters in transient analysis. It again affects the stability and accuracy of solution. For smaller time steps, good accuracy can be achieved but at the cost of increase in computational time. For present study, time step corresponding to 0.5°, 1°, 1.5° and 2° were considered and results are tabulated in Table-1.

Table 1: Variation in Numerical Efficiency with Varying Time Steps

Time Step (sec)	Corresponding runner rotation (degree)	Efficiency (%)	Duration (hours)
1.016×10^{-4}	0.5	88.05	155
2.032×10^{-4}	1.0	88.03	77
3.046×10^{-4}	1.5	79.23	52
4.064×10^{-4}	2.0	75.26	39

It is seen that efficiency increases with decrease in time step but the computational period increases. The increase in computational period for runner rotation 1 to 0.5° is nearly double but there is slight improvement in efficiency and hence value at 1° runner rotation was considered to be optimum with existing computational facility in simulations.

IX. Results And Discussions

The flow simulation has been carried out at three different discharge coefficients keeping head constant. Three values of discharge considered are 0.0807 m³/sec, 0.123m³/sec and 0.170 m³/sec corresponding to discharge coefficient of 0.050, 0.077 and 0.105 respectively to study the effect of discharge on hydrodynamic parameters of Pelton turbine. The discharge 0.123m³/sec is rated discharge.

The flow simulation has been carried out for three values of discharge at constant rated speed of 820 rpm and the results are analysed.

9.1 Variation in torque and efficiency

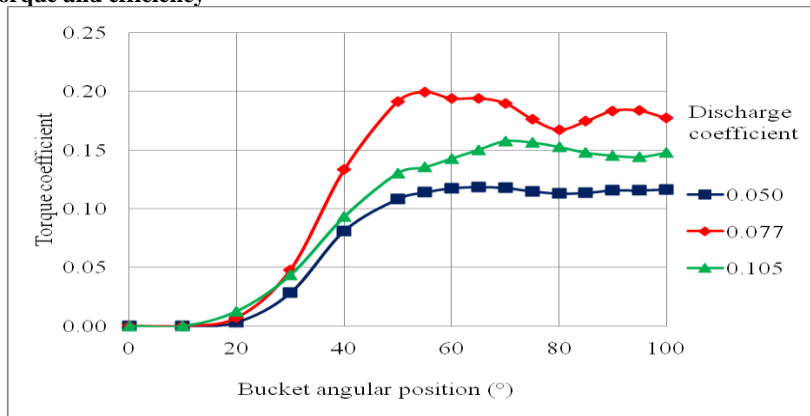


Fig 5: Variation in torque experienced by rotor for different discharge.

The variation of torque at different discharge in Fig.5 indicate that torque experienced by runner is more at rated discharge and it decreases either side. It may be due to interference to jet by buckets at more discharge and decrease in momentum at lower discharge. The fluctuation in torque is seen more at discharge coefficient of 0.077 and nearly constant at discharge coefficient of 0.050. The variation of normalised efficiency with speed coefficient has been shown graphically in Fig.6. It is seen that maximum efficiency is achieved at rated discharge coefficient of 0.077 and decreases at lower and higher discharge values.

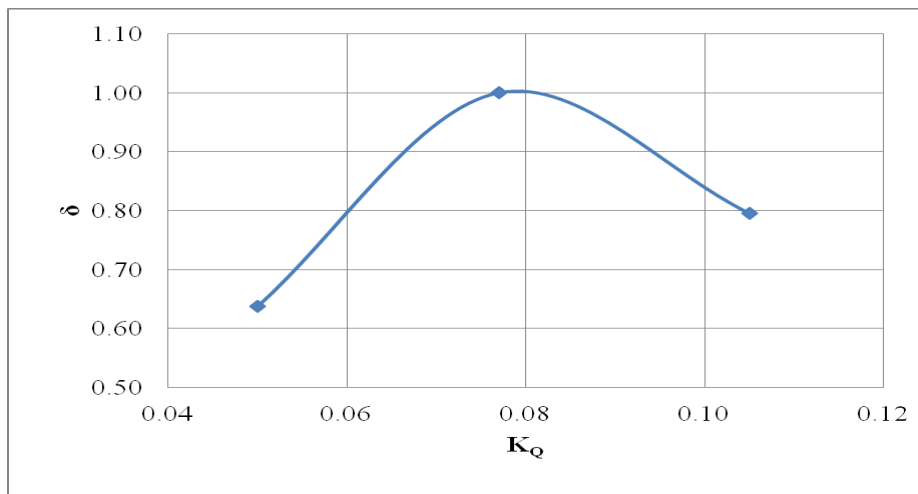


Fig. 6: Variation in normalised efficiency with discharge coefficient

9.2 Streamwise blade loading

The variations in pressure and velocity coefficients have been obtained at mid span of rotor. The stream wise variation in blade loading and velocity coefficients at 820 rpm is shown in Fig.7 to Fig.9. The maximum loading is seen for rated discharge. From Fig.7, it is observed that blade loading coefficient is uniform at mid of bucket.

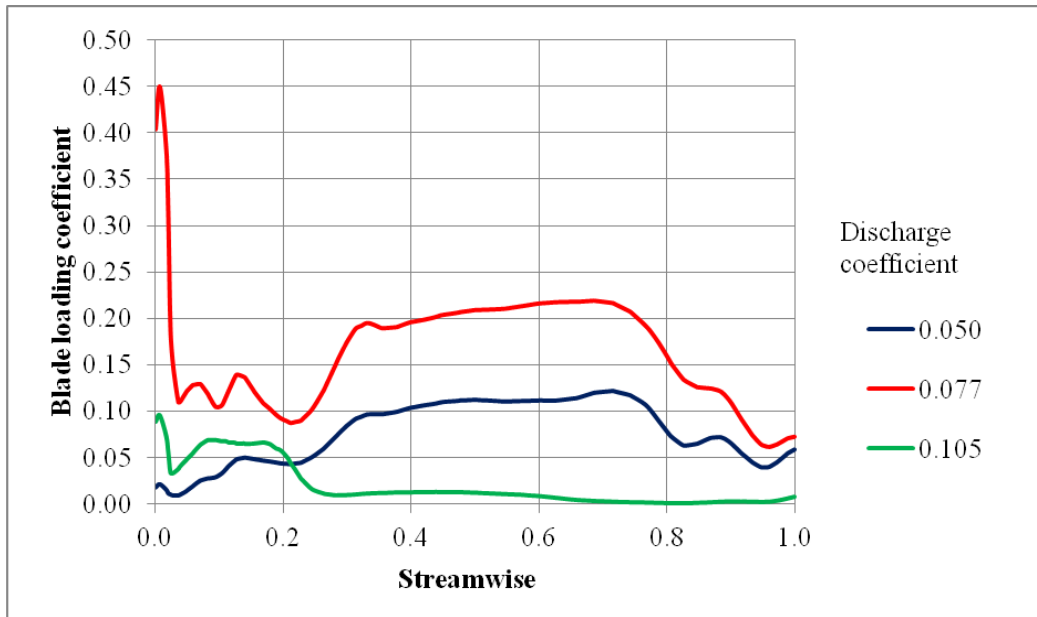


Fig. 7: Variation in blade loading for 820 rpm at mid span for different discharge

9.3 Variation in relative velocity

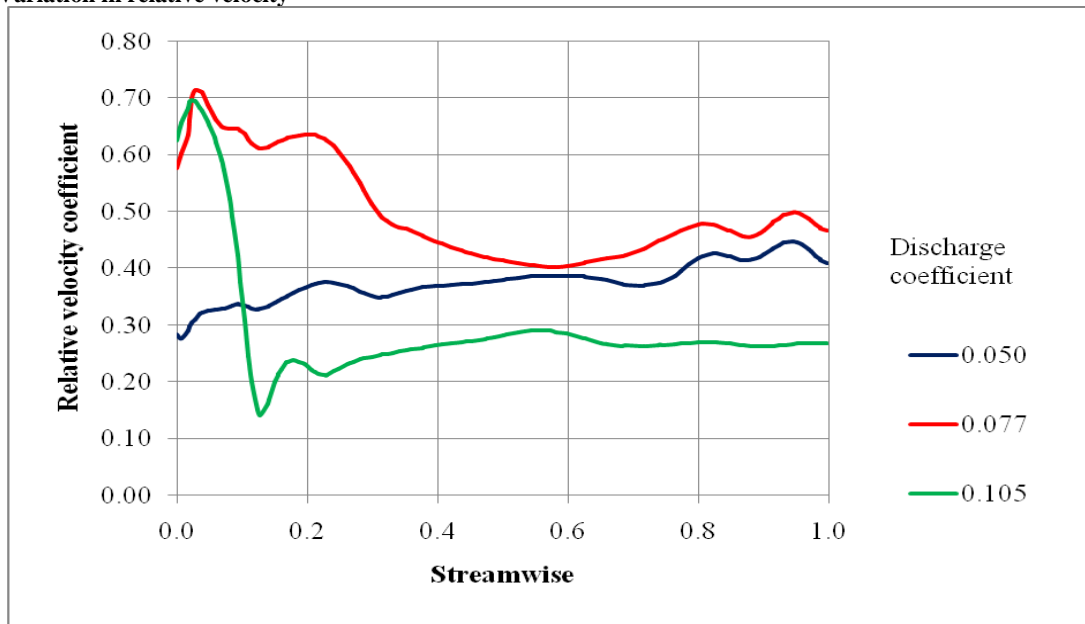


Fig. 8: Variation in relative velocity for 820 rpm at mid span for different discharge

The relative velocity variation in Fig. 8 indicates that as the discharge increases, difference in relative velocity between inlet and outlet increases and also variation is minimised.

9.4 Variation in absolute velocity

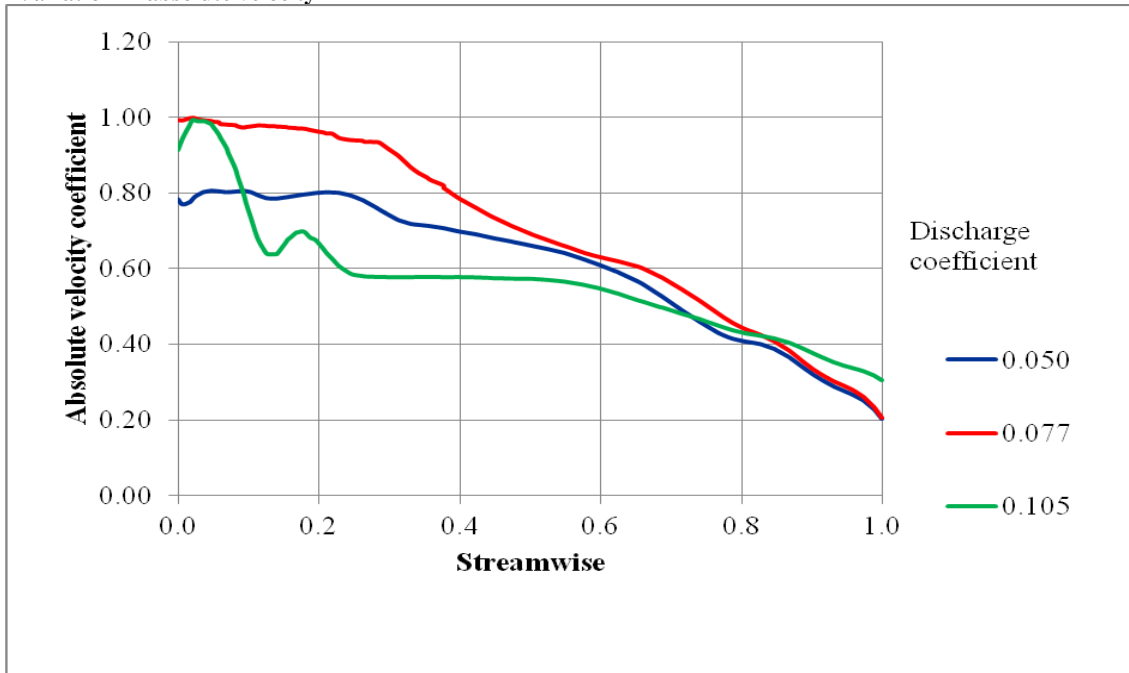


Fig.9: Variation of absolute velocity for 820 rpm at mid span for different discharge

Absolute velocity coefficient decreases gradually from inlet to outlet for all three discharges characterising features of a turbine and it is approximately same at outlet for all the cases irrespective of discharge coefficient as shown in Fig.9.

9.5 Variation in water volume fraction

As discharge varies, area of jet varies. The variation in water volume fraction at different spans with varying discharge is shown in Fig.10 to Fig.12.

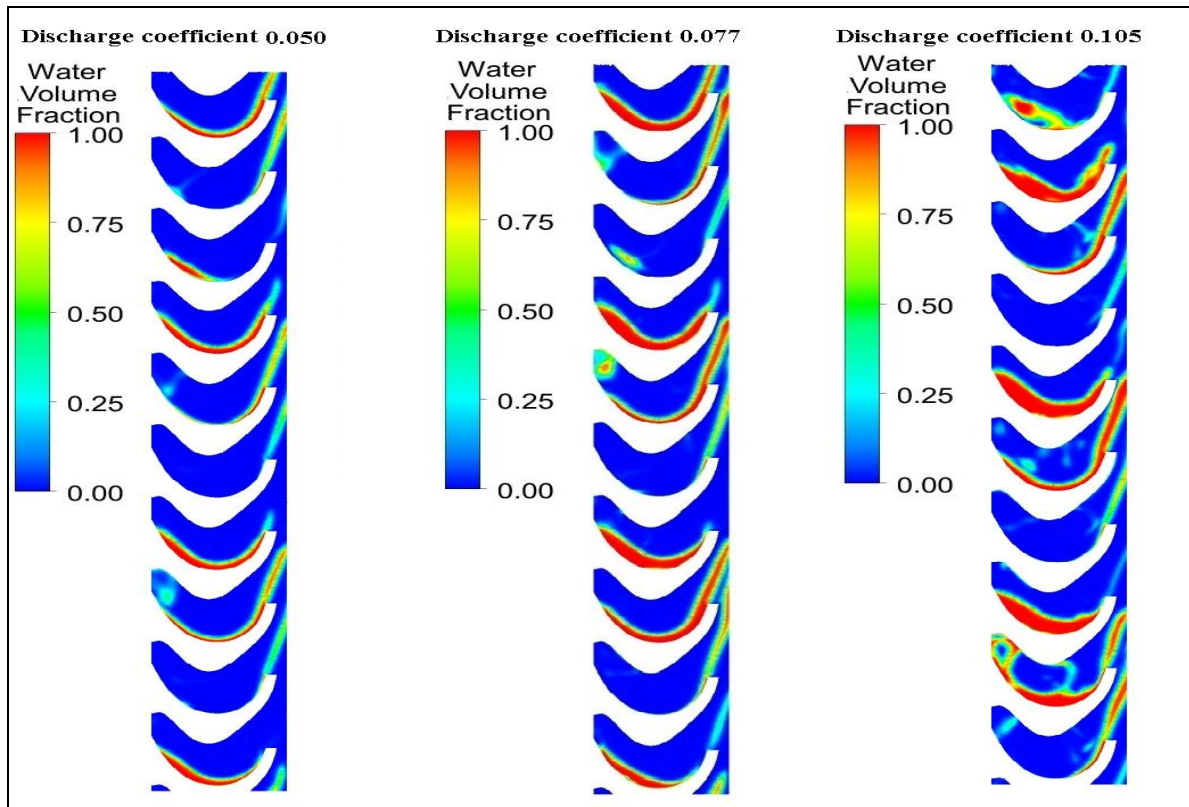


Fig 10: Variation in water volume fraction at 0.25 span for different discharge

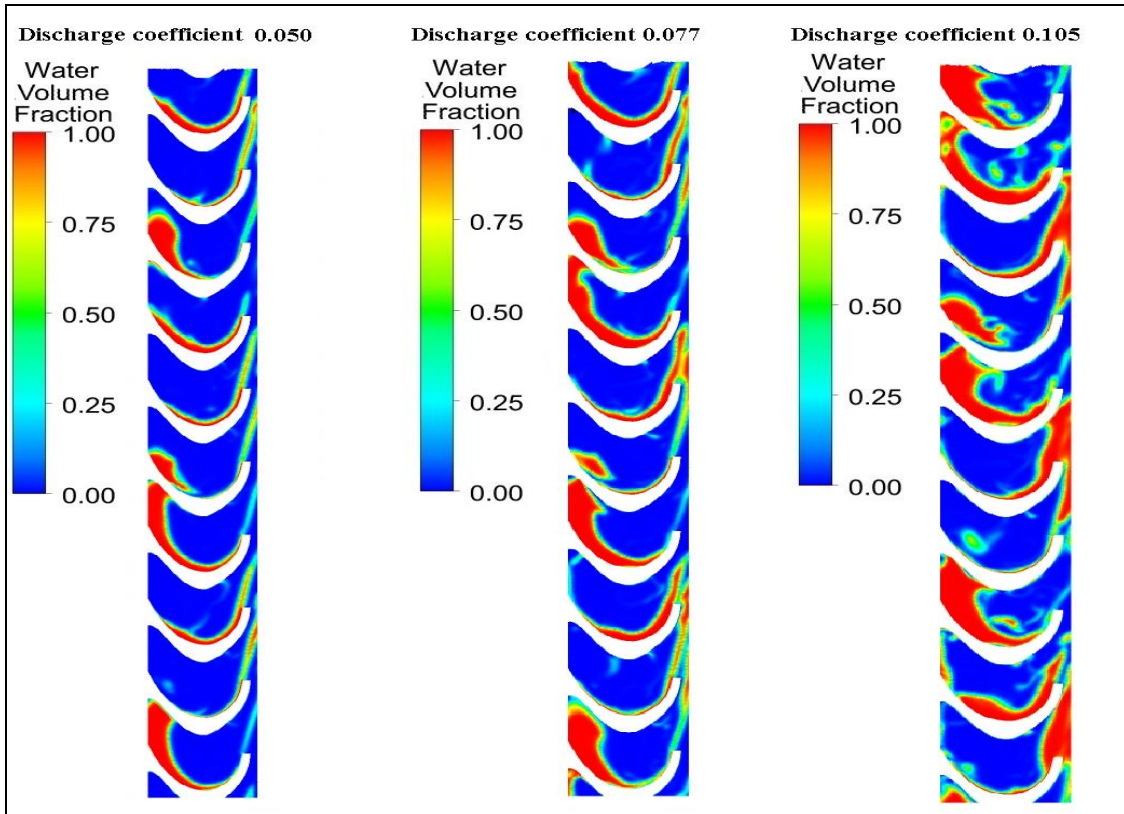


Fig 11: Variation in water volume fraction at 0.5 span for different discharge

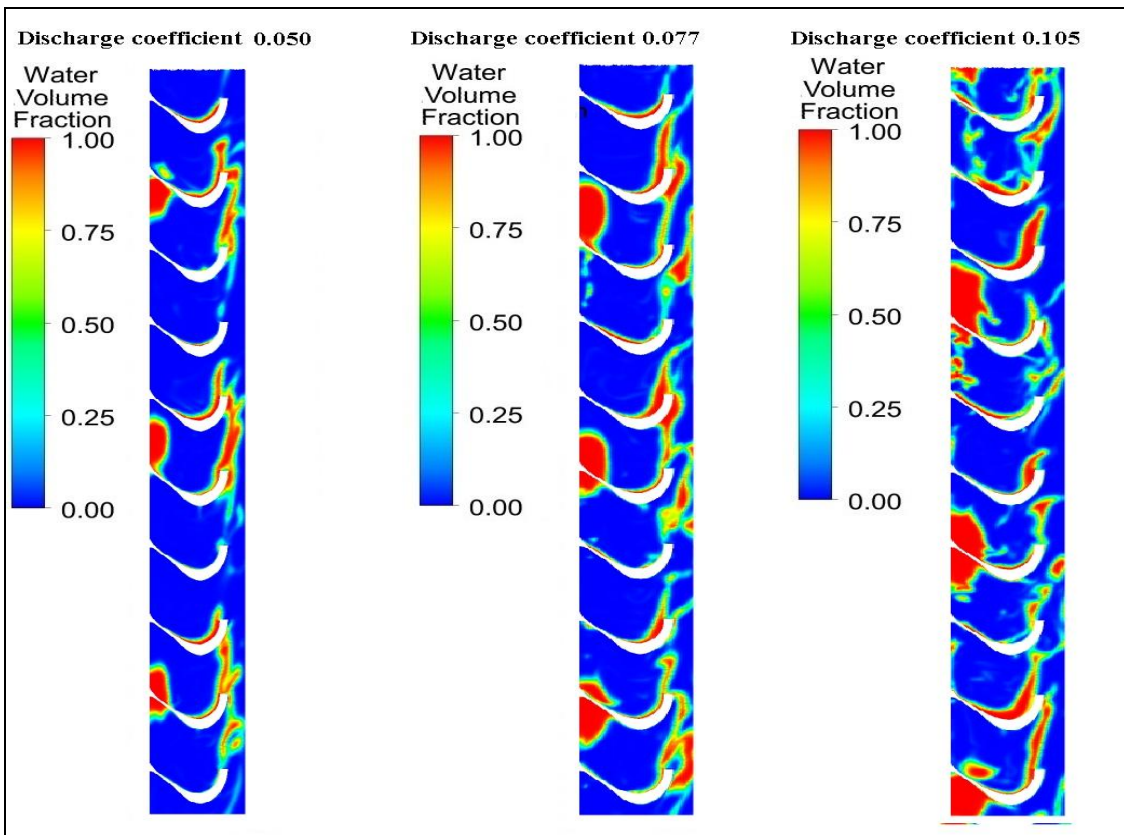


Fig.12: Variation in water volume fraction at 0.75 span for different discharge

It is seen from Fig.10 to Fig.12 that thickness of water sheet is maximum at mid span and least at 0.75 span. This indicates that jet strikes the bucket at mid span and then mostly flow axially and downside and small amount to radially inner side. The water volume fraction is also found to increase as discharge increases.

Table 2: Average values of velocity coefficients for different discharge

Velocity Triangle parameter	Discharge coefficient					
	0.050		0.077		0.105	
	Inlet	Outlet	Inlet	Outlet	Inlet	Outlet
Relative velocity coefficient	0.51	0.42	0.51	0.46	0.51	0.44
Absolute velocity coefficient	1.00	0.16	1.00	0.18	1.00	0.20
Whirl velocity coefficient	1.00	0.09	1.00	0.06	1.00	0.08
Flow angle (°)	0	17.45	0	21.10	0	23.58

From Table 2, it is observed that flow angle at outlet of bucket increases with increase in discharge coefficient. The relative velocity at outlet is found to decrease as the discharge is increased or decreased from rated value indicating more frictional loss at off-design condition. The absolute velocity at outlet is found to increase as discharge increases.

Table 3: Average values of non-dimensional parameters for different discharge

Discharge coefficient	K_T	K_L	ϕ	η (%)
0.050	0.120	0.822	0.480	56.13
0.077	0.185	0.899	0.480	88.03
0.105	0.150	0.874	0.480	70.00

The torque, loss coefficients and efficiency values shown in Table-3 indicate that the maximum values of these parameters are found to be at rated discharge.

Table 4: Water distribution at exit of runner for different discharge

Discharge coefficient	Axial (%)	Radially inward (%)	Radially outward (%)
0.050	91.00	7.68	1.32
0.077	89.93	9.09	0.98
0.105	81.76	13.88	4.36

From Table 4, it is seen that water passing axially decreases with increase in discharge coefficient. Water leaving the runner radially inward increases with increase in discharge coefficient but water passing radially outward is minimum for rated discharge.

X. Conclusion

It is seen that time step, turbulence models, mesh size affect the accuracy of numerical simulation and hence these parameter values should be chosen wisely.

It is observed that flow angle at outlet is affected by variation in discharge coefficient and found to be increasing with increase in discharge whereas whirl velocity at outlet is minimum at rated discharge and increases either side of this. The variation of relative and absolute velocity along stream at mid span gives decreasing trend from inlet to outlet at all discharges. The relative velocity at outlet is maximum at rated discharge and decreases either side of it while absolute velocity at outlet is nearly independent of discharge. The quantity of water passing axially decreases while radial flow in inward direction increases with increase in discharge but outward flow is minimum at rated discharge.

As the discharge increases, water volume fraction found to be increased at all spans and maximum water volume fraction is seen at mid spans for all discharge values. The highest value of blade loading coefficient is found out to be for rated discharge coefficient of 0.077. The torque and efficiency are found maximum at rated discharge. The frictional loss is minimum at rated discharge giving highest efficiency. Hence it is concluded from simulation results at different discharge that the best performance of turbine is achieved at rated discharge and this confirms the validity of CFD results for flow simulation of Pelton turbine.

Nomenclature

- g - acceleration due to gravity (9.8 m/s^2)
- B - bucket width (m)
- D - pitch diameter of runner (m)
- Z - No. of jets
- L - length of bucket (m)
- H - head (m)
- N - rotational speed of rotor (rpm)
- P_O - numerical power output (Watt)
- P_I - power input (Watt)
- Q - volume flow rate of fluid at jet inlet (m^3/s)
- T - torque on runner (N-m)
- ρ - density of water at 20°C (997 kg/m^3)
- η_H - hydraulic efficiency (%)
- C_P - blade loading coefficient
- T - torque (N-m)

W - relative velocity (m/s)
C - absolute velocity (m/s)

Subscript 1 and 2 denotes the values of parameter at inlet and outlet of bucket. Subscript m denotes values of mixture.

References

- [1]. V.V. Barlit, P. Krishnamachar, M.M. Deshmukh, Adarsh Swaroop and V.K. Gehlot, Hydraulic turbines- volume I and II (MACT, Bhopal, 1983.)
- [2]. P.N. Modi and S.M. Seth, Hydraulics and fluid mechanics including hydraulic machines (Standard Book House, Delhi, 2011)
- [3]. J. Lal, Hydraulic machines including fluidics (Metropolitan Book Company, New Delhi, 2007)
- [4]. J.D. Desai, V.A. Soni, V.K. Chauhan, S.S. Charania and K.C. Patel, Evaluation of twin jet Pelton turbine using CFD, Proceedings of Thirty Ninth National Conference on Fluid Mechanics and Fluid Power, Gujarat, India, 2012, 194-197.
- [5]. V Gupta, V Prasad and R Khare, Numerical modeling for hydro energy convertor: Impulse turbine, Proceedings of International Conference on Global Scenario in Energy & Environment, Bhopal, India 2013.
- [6]. M Francois, G Vuillerod, Development and recent projects for hooped Pelton turbine, Proceedings of Hydro-2002, Turkey. 4-7 Nov 2002
- [7]. A Perrig, F Avellan, J.L. Kueny and M Farhat, Flow in a Pelton turbine bucket: Numerical and experimental investigations, Transaction of ASME, 128, 2006, 350- 358.
- [8]. B Zoppe, C Pellone, T Maitre and P. Leroy, Flow analysis inside a Pelton turbine bucket, Transaction of ASME, 128, 2006, 500-511.
- [9]. V Gupta and V Prasad, Numerical investigations for jet flow characteristics on Pelton turbine bucket, International Journal of Emerging Technology and Advanced Engineering 2(7), 2012, 364-370.
- [10]. E Parkinson, C Neury, H Garcin, G Vulllioud and T Weiss, Unsteady analysis of Pelton runner with flow and mechanical simulations (Hydropower & Dams, 2006).
- [11]. T Patel, B Patel, M Yadav and T Foggia, Development of Pelton turbine using numerical simulation, Proceeding of 25th IAHR Symposium on Hydraulic Machinery and Systems. IOP Conf. Series: Earth and Environmental Science 12. 2010.
- [12]. P Dynampally and VS Rao, CFD analysis of Pelton turbine, Proceedings of Thirty Ninth National Conference on Fluid Mechanics and Fluid Power, Gujarat, India, 2012 pp 58.
- [13]. MS Konnur and K Patel, Numerical analysis of water jet on flat plate, Proceeding of National Conference on Fluid Mechanics and Fluid Power, Raipur, India, 2006.
- [14]. AKMK Islam, S Bhuyan and FA Chowdhury, Advanced composite Pelton wheel design and study its performance for pico/micro hydro power plant application, International Journal of Engineering and Innovative Technology, 2 (11), 2013, 126-132.
- [15]. Y X Xiao, C J Zeng, J Zhang, Z G Yan and Z W Wan, Numerical analysis of the bucket surface roughness effects in Pelton turbine, Proceeding of 6th International Conference on Pumps and Fans with Compressors and Wind Turbines. IOP Conf. Series: Materials Science and Engineering 52 (2013) 052032
- [16]. Zh Zhang, Flow friction theorem of Pelton turbine hydraulics, Journal of Power and Energy, 221(Part A), 2007, 1173-1180.
- [17]. Zh Zhang, Analytical method for frictional flows in a Pelton turbine, Journal of Power and Energy 223(Part A), 2009, 597-608.
- [18]. Zh Zhang, Inlet flow conditions and jet impact work in a Pelton turbine, Journal of Power and Energy, 223(Part A), 2009 589-596.
- [19]. Zh Zhang, Flow dynamics of free surface flow in the rotating buckets of a Pelton turbine, Journal of Power and Energy, 223 (Part A), 2009, 609-623.
- [20]. Zh Zhang, Flow interactions in a Pelton Turbines and the hydraulic efficiency of the turbine system, Journal of Power and Energy, 221 (Part A), 2007, 343-357.
- [21]. KC Binaya and Bhola Thapa, Pressure Distribution at inner surface of selected Pelton bucket for midro hydro, Journal of Science, Engineering and Technology 5(2), 2009, 42-50.
- [22]. A Santolin, G Cavazzini, G Ardizzon and G Pavesi, Numerical investigation of the interaction between jet and bucket in a Pelton turbine, Proceedings of the Institution of Mechanical Engineers, Journal of Power and Energy 223, 2006, 721-728
- [23]. D Jost, P Meznar and A Lipej, Numerical prediction of Pelton turbine efficiency, Proceeding of 25th IAHR Symposium on Hydraulic Machinery and Systems, IOP Conf. Series: Earth and Environmental Science-12. 2010.
- [24]. D Benzon, A Židonis, A Panagiotopoulos, GA Aggidis, JS Anagnostopoulos and DE Papanonis, Impulse turbine injector design improvement using Computational Fluid Dynamics, Journal of Fluid Engineering, Transaction of ASME. 2014.
- [25]. M Manohar and P Krishnamachar, Fluid Mechanics Volume II, (Vikas Publishing House Pvt. Ltd., New Delhi, 1983)
- [26]. Anderson John D. Computational Fluid Dynamics (McGraw-Hill Inc. New York, 1995).
- [27]. ANSYS CFX 13.0 software manual.